

# Nano satellite “ITF-2” developed by University of Tsukuba YUI project

By Atsushi YASUDA<sup>1)</sup>, Akihiro NAGATA<sup>2)</sup>, Hiromasa WATANABE,<sup>1)</sup> and Toshihiro KAMEDA<sup>3)</sup>

<sup>1)</sup>Graduate School of Pure and Applied Sciences, University of Tsukuba, Tsukuba, Japan

<sup>2)</sup>Graduate School of Systems and Information Engineering, University of Tsukuba, Tsukuba, Japan

<sup>3)</sup>Faculty of Engineering, Information and Systems, University of Tsukuba, Tsukuba, Japan

(Received June 21st, 2017)

ITF-2, which was developed by the University of Tsukuba YUI project, was designed based on ITF-1. ITF-1 was the first CubeSat at the University of Tsukuba; however, signals were never received. Although ITF-2 was developed based on ITF-1, the components that resulted in failure were reconsidered and improved for use in ITF-2. In this paper, the overview, subsystems of ITF-2, and the design improvement from ITF-1 to ITF-2 are presented. In addition, ITF-2 was deployed from “Kibo” on January 16, 2017 and it is still operational as of September 2017. This paper reports the operation results and the achievement of missions: “YUI network”, which is a “participatory” mission using CubeSat, involving participation from people around the world, ultra-small antenna, which is used for two amateur bands by attaching it to a metal structure, and a new microcontroller, which has been reported to be saving energy, high radiation resistant and demonstrated to acquire a new achievement in space. The operation results as of September 2017 indicate that more than 900 reception reports from 19 countries were reported, indicating the success of the outreach.

**Key Words:** Nano-satellite, CubeSat, ISS-deployed satellite, Amateur radio satellite

## 1. Introduction

The University of Tsukuba YUI project<sup>1)</sup>, a small satellite development project set up in 2011, has developed two CubeSats, Imagine The Future-1 (ITF-1) and Imagine The Future-2 (ITF-2). ITF-1 was launched by the H-IIA rocket from the Tanegashima Space Center on February 28, 2014. However, no signal has been received from it and its operation completed upon reentry on June 29, 2014. Subsequently, the development of a second CubeSat ITF-2 was started. ITF-2 is a 1U-sized CubeSat based on the design of ITF-1; however, it improved on the defects of ITF-1. The development of ITF-2 was completed in March 2016. ITF-2 was loaded on the “KOUNOTORI” H-II Transfer Vehicle and launched from the Tanegashima Space Center by the H-IIB rocket on December 9, 2016. On January 16, 2017, ITF-2 was deployed from “Kibo”, the Japanese experiment module at the International Space Station (ISS), by using JEM Small Satellite Orbital Deployer (J-SSOD) system<sup>2)</sup>. J-SSOD is the deployment mechanism developed by JAXA to deploy micro/nano-satellites from Kibo. We succeeded in receiving signal and communication from ITF-2 at the University of Tsukuba ground station within one day after the deployment. By April 2017, we finished checking ITF-2 soundness, and the operation to achieve its main mission, including education and amateur radio, started.

In this paper, an overview and systems of ITF-2 as well as design improvements from ITF-1 will be presented. ITF-2 consists of five systems, namely power supply, command and data handling (C&Dh), communication, thermal and structure, and attitude control system. The development of ITF-2 was mainly based on ITF-1; however, we referred to other satellite projects such as HORYU-II<sup>3)</sup> and XI-V<sup>4)</sup> for analysis methods, power supply balance analysis<sup>5)</sup> and the design of ITF-2, and

the attitude control system<sup>4)</sup>. The defects and the process of improvement must be the precept for incoming nanosatellites. Furthermore, ITF-2 has three missions. “The construction of the YUI network”, the main mission, provides a unique use for university CubeSats. Nearly all CubeSats developed by universities were mainly used for scientific and technical missions. This mission is the “participatory” mission for this, which aims to promote public interest in space and satellite, and interaction through opportunities for receiving signals from ITF-2. In terms of technical missions, ITF-2 demonstrates an “ultra-small antenna”: the plate antenna for CubeSat, which is used by attaching it on a metal panel directly and as redundancy for communication, was verified in space for the first time, and energy saving, high radiation resistant type “FRAM microcontroller”. The results of ITF-2 operation and the present status of achievement of these missions will also be reported.

Figure 1 shows the appearance of the ITF-2 flight model and Table 1 presents an overview of ITF-2. It transmits telemetry data and messages using amateur radio band (430 MHz). Its orbital inclination is 51.6° and its altitude is approximately 400 km. CW and FM data formats are published on ITF-2 operation web page<sup>6)</sup>. In September 2014, ITF-2 was selected as one of the nanosatellites deployed from Kibo.

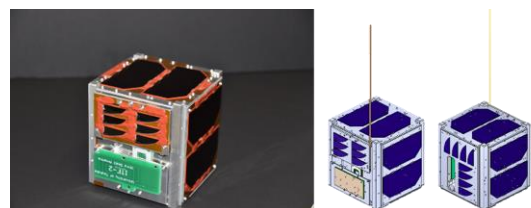


Fig. 1. ITF-2 Flight Model.

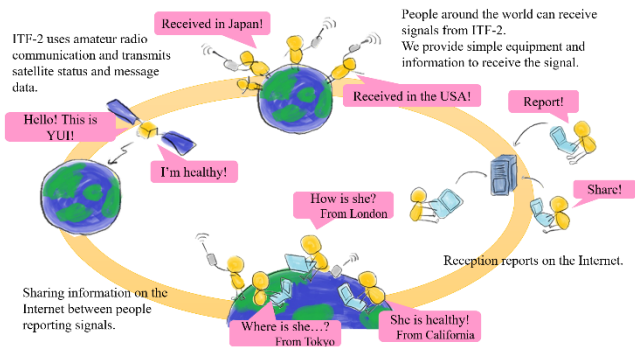


Fig. 2. YUI network

Table 1. Overview of ITF-2.

Name	ITF-2 (Imagine The Future-2) Nickname: YUI 2
Size	111.5 mm x 110 mm x 115.5 mm
Wight	1.39 kg
Downlink	437.525 MHz (monopole antenna, ultra-small antenna)
Uplink	Wave types: A1A, F2A, F2D (1200 bps) 430 MHz (monopole antenna, ultra-small antenna); AFSK (AX.25, 1200 bps) 144 MHz (ultra-small antenna): AFSK (AX.25, 1200 bps)
Receiver	NISHI MUSEN Receiver for Nano-satellite 301A
OBC	PIC16F877, MSP430FR5739, ATMEGA2560
Attitude control	Permanent magnet, Magnetic damper (Passive control with earth magnetism)
Battery	Li-ion battery
Solar cell	40 x 80 mm Triple Junction (TJ) GaAs Solar cells Triangle TJ GaAs solar cells

## 2. ITF-2

### 2.2. Missions

#### 2.2.1. Development of YUI network

Nearly all CubeSats developed by universities had technical, scientific, and observational missions. Although there are diverse applications of a CubeSat, however, it is not common to use a CubeSat developed by a university as the main mission, which is a participatory mission for the public, including children and adults, and aims to promote interest in space and satellite, and interact globally with a CubeSat. Thus, the YUI project proposed the “YUI network” as a new mission achieved through the participation of many people around the world.

Figure 2 shows the conceptual scheme of the “YUI network”. The YUI network is a very innovative and challenging concept of network, which is formed by connecting people who may not have any relationship except receiving signals from ITF-2. This promotes international exchange, education for science and engineering, and amateur radio activities. It will also inspire interest in science. The YUI project provides opportunities to connect, e.g., in receiving events for kids and on the Internet.

#### 2.2.2. Demonstration of new microcontroller

In the design of a satellite, it is necessary to consider cosmic rays, which have negative effects on microcontrollers loaded on the satellite, such as single event latch-up (SEL) and single event upset (SEU). These lead to damage to microcontrollers or decrease the reliability of storing data.

Recently, ferroelectric RAM (FRAM) microcontrollers have been marketed with the claim that they have high radiation resistance compared to conventional flash microcontrollers.

In this mission, ITF-2 was loaded with a FRAM microcontroller, MSP430FR5739 (MSP). For this mission, the number of SEL and SEU events of MSP were counted. MSP monitors whether SEU, that is, illegal bit flips occurred or not, every 1 s. In addition, the main microcontroller (which will be presented in section 2.3.3) monitors the current of the MSP and counts the number of SEL occurrences when the current is greater than a threshold value. Finally, the result will be compared with that of radiation testing. This demonstration leads to increased choices for microcontrollers for satellite.

#### 2.2.3. Demonstration of ultra-small antenna

The size of the 1U CubeSat was approximately 10 cm<sup>3</sup> and many CubeSats uses amateur band for communication. If, for example, the 1U CubeSat uses amateur band, such as the 430 MHz band, generally a monopole antenna with a length of approximately 17 cm, and a deployment mechanism to store the antenna are needed. However, there are many risks that cause accidents when deploying an antenna, such as vibration from rocket or shock when the satellite itself deploys. This leads to reduced reliability of the communication system.

The ultra-small antenna (Fig. 3) is one solution to improve reliability. The frequency of this antenna was 430 MHz and 144 MHz band. The antenna size was approximately 3 cm x 6 cm and the type was an inverted-F antenna. This type of antenna is used for the amateur band and has not been demonstrated for space application. Figure 4 shows the ultra-small antenna pattern of the 435 MHz band. In Fig. 4, 0 dB indicates the maximum gain of the ultra-small antenna. The value obtained by adding about 23 dB to 0 dB shown in Fig. 4 is 0 dBi. Figure 5 shows the SWR spectrum of the ultra-small antenna. The SWR was 4.16 for the 144 MHz band and 1.68 for the 430 MHz band.

The merits of this antenna are that it does not require an antenna development mechanism and can be used by attaching it to a metal surface. Radio waves are reflected by metal and this property has a negative effect on communication using an antenna on metal panel. Most CubeSats are made of metal; however, the ultra-small antenna can be used by attaching it directly to a metal panel. In this mission, the uplink of the 144 MHz band from the University of Tsukuba ground station and the downlink of the 430 MHz band from ITF-2 were confirmed.

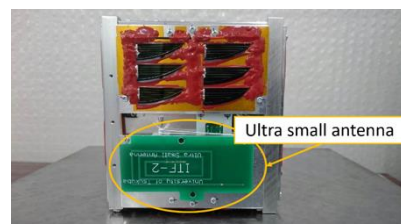


Fig. 3. Ultra-small antenna.

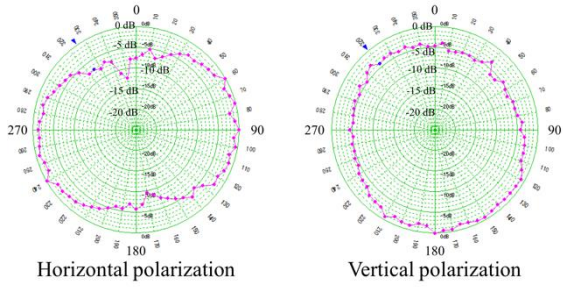


Fig. 4. Ultra-small antenna pattern. Left: horizontal polarization, Right: vertical polarization. 0 dB indicates the maximum gain of the ultra-small antenna. The value obtained by adding about 23 dB to 0 dB shown in Fig. 4 is 0 dBi.

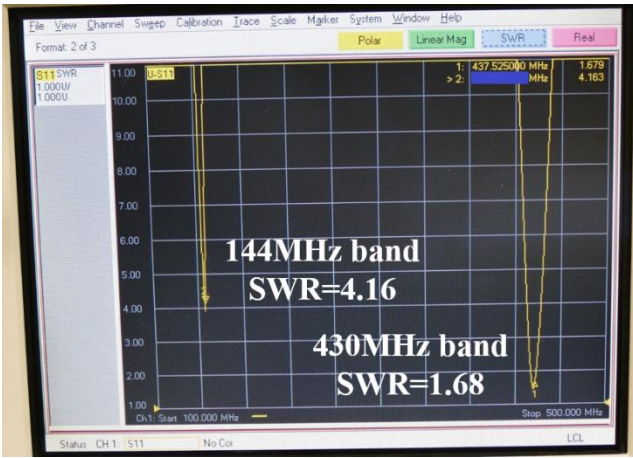


Fig. 5. SWR of ultra-small antenna. SWR is 4.16 for 144 MHz band and 1.68 for 430 MHz band.

### 2.3. Subsystems

Figure 6 shows the subsystems of ITF-2. ITF-2 consists of five subsystems, namely power supply, thermal and structure, command and data handling (C&Dh), communication, and attitude control systems. In this section, each subsystem will be introduced.

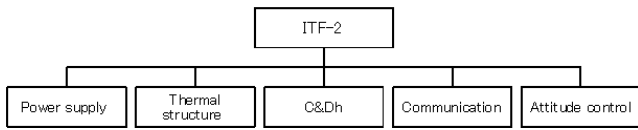


Fig. 6. ITF-2 subsystem.

#### 2.3.1. Power supply system

ITF-2 loads two types of solar cells: the 40 mm x 80 mm triple junction (TJ) GaAs solar cell and the triangle TJ GaAs solar cell. The cost of triangle cells per one cell is approximately forty times smaller than that of 40 mm x 80 mm cells. The connection of TJ solar cells are two serials and a parallel on  $\pm Y$  and  $\pm Z$  panels. Figure 7 shows the connection of solar cells on each panel. The connection of triangle solar cells are two serials and two parallels on  $-X$  panel, and two serials and four parallels on  $+X$  panel. Figures 8, 9, and 10 shows the I-V and W-V curves of the solar cells.

The power balance analysis is based on Ref. 5 and the following condition was considered: the worst satellite rotating

condition is that the solar cells generate the lowest electric power when ITF-2 rotates around the Z axis (or Y axis);  $\pm Y$  and  $\pm X$  (or  $\pm Z$  and  $\pm X$ ) panels receive sunlight, assuming that the angle between the solar light and the normal line of each panel changes by 1 degree per 1 minute (Fig. 11). Based on this condition, the average generated power was calculated as follows.

- (1) Calculate the angle  $\theta$  between the solar light and normal lines of each panel at a certain time.
- (2) Calculate the generated power  $P$  of each panel with Eq. (1).

$$P = I \times V \times \cos\theta, \quad (1)$$

where  $I$  is the short circuit current of each panel and  $V$  is the voltage. From Figs. 8, 9, and 10,  $I$  of  $\pm Y$  (or  $\pm Z$ ),  $+X$ , and  $-X$  panel were 500 mA, 170 mA, and 120 mA, respectively, while  $V$  was 4.4 V.

- (3) The generated power of the satellite in a certain time was calculated by summing the generated power of each panel.
- (4) The average generated power was calculated by dividing the sum of generated power until a certain time by the time.

Figure 12 shows the result of this calculation. The average generated power converged to 1.84 W. Table 2 presents ITF-2 Flight Model power consumption for each operation mode. ITF-2 usually repeats the routine that it transmits CW for 10 s and receives signals for 90 s. This operation is defined as “normal transmission”. From Table 2, the average consumption power of the normal transmission was  $0.87 \times 0.9 + 1.47 \times 0.1 = 0.93$  W. In addition, the heater works when the temperature of the battery is below  $5^\circ\text{C}$  and the heater consumption power was 0.3 W. It was assumed that the minimum sunshine rate was 62%, the time to go around the Earth was 92 min and the heater works for 15 min per round of the Earth. The consumed electric energy (Wh) for normal transmission per round of the Earth was  $0.93 \times 92 / 60 + 0.3 \times 15 / 60 = 1.50$  Wh and the generated electric energy per round of the Earth was  $1.84 \times 92 \times 0.62 / 60 = 1.73$  Wh. Thus, the amount of electric energy per round of the Earth provided to the battery was 0.23 Wh.

ITF-2 loads a consumer Li-ion battery. Figure 13 shows the discharge curves of 0.1 C (=310 mA) and 0.5 C (=1600 mA).

Figure 14 shows the system block diagram of the power supply system. To prevent ITF-2 circuit from connecting before the deployment, deployment switches and an RBF pin were loaded on ITF-2. The RBF pin was removed before launch, and the deployment switches were opened after the deployment; thus, all circuits were connected. Three DC/DC converters were loaded on ITF-2: one DC/DC converter always provides power to the receiver of communication system B.

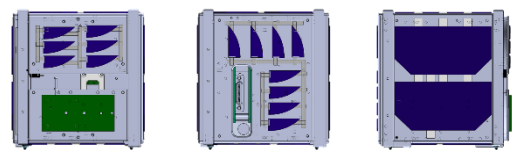


Fig. 7. Connection of solar cells on each panel. Left:  $-X$  panel, center:  $+X$  panel, and Right:  $\pm Y$  and  $\pm Z$  panels.

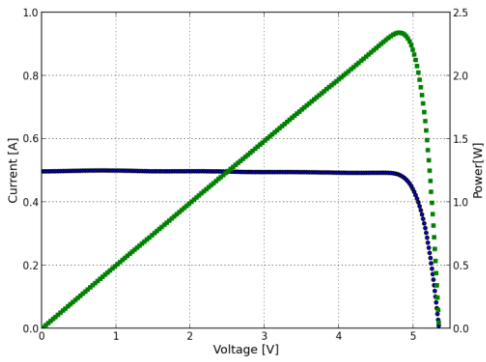


Fig. 8. I-V (blue) and W-V (green) curves of  $\pm Y$  and  $\pm Z$  panels of Flight Model.

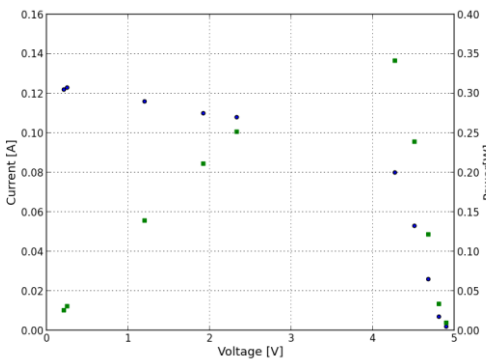


Fig. 9. I-V (blue) and W-V (green) curves of +X panel of Flight Model.

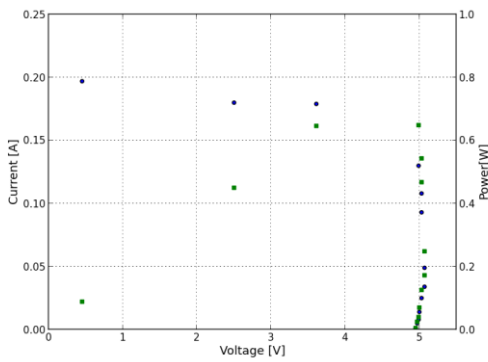


Fig. 10. I-V (blue) and W-V (green) curve of -X panel of Flight Model.

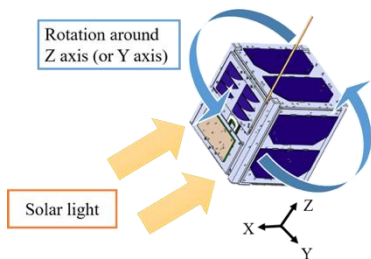


Fig. 11. Rotation of ITF-2 under the condition of power analysis:  $\pm Y$  and  $\pm X$  panels (or  $\pm Z$  and  $\pm X$  panels) receive solar light and by assuming that the angle between the solar light and the normal line of each satellite panel changes by 1 degree per 1 minute.

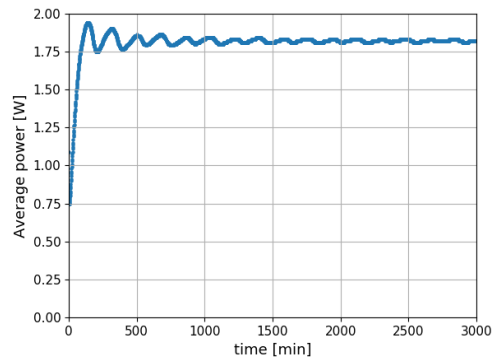


Fig. 12. Result of power analysis. Plots show the calculation of the total generated power divided by each time. The average generated power converged to 1.84 W.

Table 2. Flight Model power consumption of each operation mode.

Mode	Power consumption [W]
Receive	0.87
CW(A1A)	1.47
F2A	4.70
F2D	4.13
Normal transmission (A1A : Receive = 1 : 9)	0.93
Heater	0.30

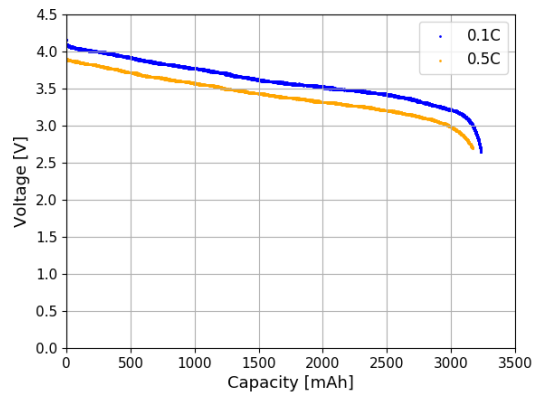


Fig. 13. Battery discharge curves of Flight Model. The blue curve shows 0.1 C (=310 mA) and the orange curve shows 0.5 C (=1600 mA).

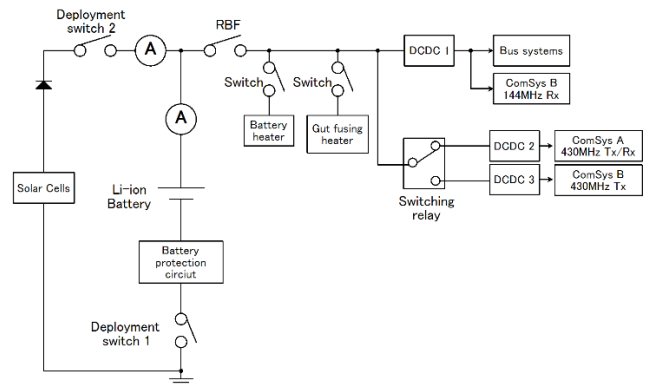


Fig. 14. System block diagram of power supply system of ITF-2.



### 2.3.2. Thermal and structure system

The most severe device for temperature on ITF-2 is the battery. Thus, two thermal sensors and a battery heater were loaded on as a thermal controller (Fig.15). ITF-2 determines the battery temperature by averaging the values measured by these sensors. A copper wire was wound on the battery as a heater and this heater works when the temperature of the battery drops to below 5 °C because the operating temperature range of the battery is between 0–40 °C. Moreover, thermal sensors were also loaded on ±Y and ±Z panels to monitor the temperature of the satellite body in space.

The ITF-2 body structure was made of aluminum. The antenna deployment mechanism was loaded on the -X panel. The monopole antenna was wound as shown Fig. 16 with an antenna restriction wire. After 30 min from deployment at the ISS, the nichrome wire was heated, then the restriction wire was burnt out and the monopole antenna was deployed. In terms of the Flight Model, the measured average electric power to burn out the wire was 5.15 W and the measured time was approximately 20 s. Such an antenna deployment mechanism was also used by other CubeSats<sup>5)</sup>.

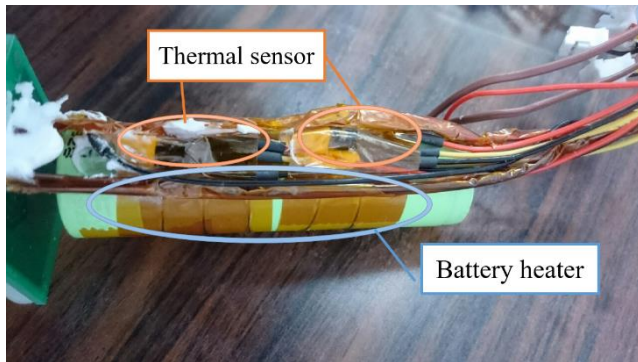


Fig. 15. Two thermal sensors and battery heater on battery.

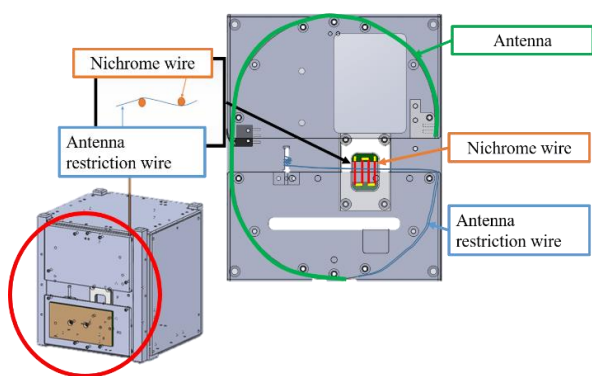


Fig. 16. ITF-2 Antenna deployment mechanism

### 2.3.3. Communication system and C&Dh system

Figure 17 shows the communication system block diagram. Figure 18 shows the placement of the antennas. ITF-2 transmits and receives signals with the monopole antenna (430 MHz band) and the ultra-small antenna (430 MHz and 144 MHz bands). ITF-2 has two communication systems: system A, which connects to the monopole antenna and system B, which connects to the ultra-small antenna. ITF-2 downlinks radio

waves, including A1A, F2A, and F2D, which are popular for amateur radio. As mentioned in section 2.3.1, the normal transmission (10 s transmission and 90 s standby) is the basic downlink cycle. The transmission of F2A and F2D are customized by the uplink commands. During the basic downlink cycle, ITF-2 transmits housekeeping (HK) data, such as battery voltage, satellite temperature, and consumption current. Table 3 presents the correspondence between radio waves and downlink contents. It is possible to change downlink messages by means of an uplink. ITF-2 changes communication systems with a switching relay, such that only one side of the transmitter (TX) transmits the signal and the other side of TX is turned off. The switching cycle of the system was 50 min by default. It can be changed by means of an uplink and set one communication system continuously.

Table 3. Types of radio wave of ITF-2

Radio wave	Downlinks
CW (A1A)	HK data
F2A	HK data, message data
F2D	HK data, message data and mission data
	Mission data: the number of SEL and SEU of MSP430FR5739.

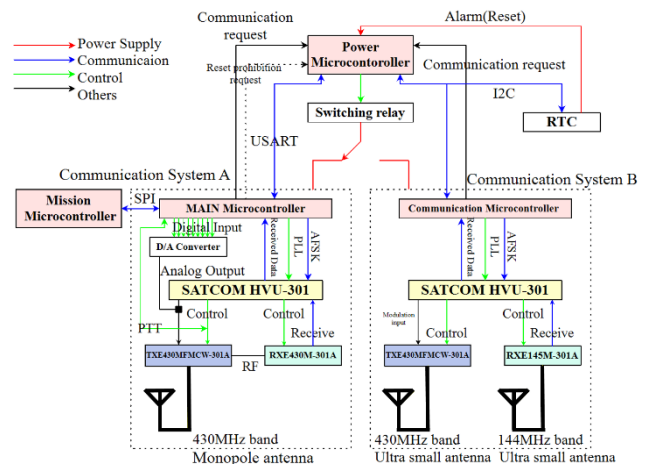


Fig. 17. Communication system block diagram of ITF-2.

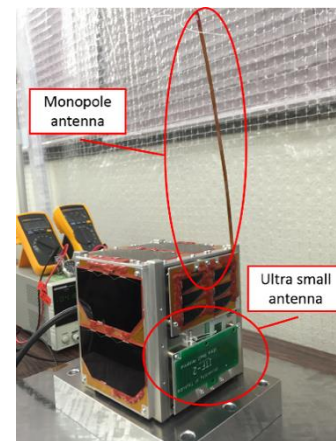


Fig. 18. Placement of ITF-2 antennas.

### 2.3.4. Attitude control system

Two magnetic dampers and a permanent magnet were mounted on ITF-2 for passive attitude control. The permanent magnet enables the satellite to determine whether the direction of the magnet and the Earth's magnetism are parallel. The permanent magnet was set parallel to the X axis to take an attitude that gives sufficient signal intensity to receive signal from the University of Tsukuba ground station and large area of solar cells to allow sunlight at very low temperature. The magnetic dampers were set parallel to the Y axis and Z axis and this resulted in the reduction of vibration around the X axis by converting the vibration to thermal energy. Figure 19 shows the placement of the magnetic dampers and permanent magnet. This technique has some advantages; it does not require any electric power and it decreases the risk of loss of satellite function due to damage in the attitude control system. The method of using the magnetic damper and permanent magnet is also used by other CubeSats<sup>4)</sup>.

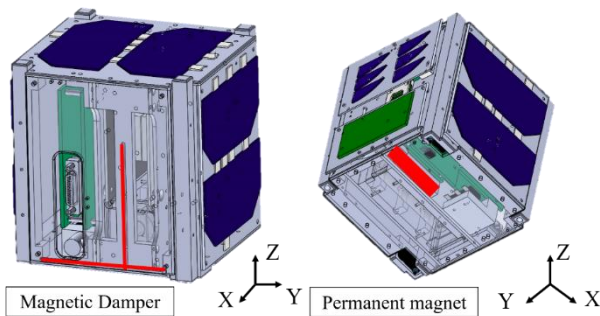


Fig. 19. Placement of ITF-2 attitude control components.

## 2.4. Design improvement from ITF-1 to ITF-2

Despite the fact that ITF-1 passed the safety review, no signal was received from it. Therefore, the designs for the components (antenna deployment mechanism, receiver, microcontroller, deployment switch, flight pin, DC/DC converter, battery and solar cells) were reconsidered to determine if these potentially contributed to the malfunction. In this subsection, the reconsideration of the ITF-1 design and the improvements in ITF-2 will be introduced.

### 2.4.1. Antenna deployment mechanism

On the antenna deployment mechanism, the possibility of not having a signal is due failure to deploy the antenna. The monopole antenna of ITF-1 was stored in the structure as shown in Fig. 20. In the antenna deployment operational test, this antenna had been caught in the body occasionally. After this, countermeasures were implemented; however, the antenna could have been caught and not deployed normally. In addition, an antenna restriction wire was wound on a resistor. Thus, it was considered that this wire slid and separated during the rocket launch.

As shown in Fig. 16, the antenna deployment mechanism of ITF-2 was loaded outside of the structure and the method to tie an antenna restriction wire was improved such that the wire was

completely burnt out.



Fig. 20. Antenna deployment mechanism of ITF-1

### 2.4.2. Receiver

Three consumer receivers were loaded on ITF-1 and the cases to hold the receivers were self-produced (Fig. 21). The resistance of the receivers against vibration was checked and the test for the Flight Model was successful; however, these were broken in the test of the Engineering Model. The types of vibration tests were the Qualification Test (QT) at the Engineering Model and the Acceptance Test (AT) at the Flight Model. The vibration of AT is the same level test as rocket vibration and QT is a stronger test than AT. Of course, the defects had been improved at that time and had cleared the QT; therefore, it was considered that these receivers broke during the launch.

Two receivers, which are the same type of receivers that have been used several times in space, were loaded on ITF-2 to increase the reliability of the communication system. The performance of the receivers was checked carefully at each development phase.



Fig. 21. ITF-1 receivers

### 2.4.3. Microcontroller

Figure 22 shows the ITF-1 communication system block diagram. The mission microcontroller (FRAM) was set in the transmission system, and the damage to this microcontroller resulted in the failure of the entire transmission system. In addition, the main microcontroller in Fig. 20 controlled the entire transmission system and this was the single-point of failure.

The mission microcontroller of ITF-2 was not set in the transmission system as shown in Fig. 17 such that it did not influence the transmission system. In Fig. 17, the power microcontroller controlled both communication system. Signals can be transmitted if NISI MUSEN, SATCOM, and power supply system would be alive, even though the power

microcontroller could be damaged.

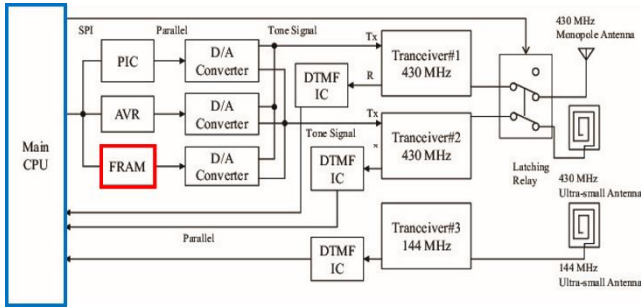


Fig. 22. ITF-1 communication system block diagram. Red square shows mission microcontroller and blue square shows main microcontroller.

**2.4.4. Deployment switch**

Figure 23 shows the ITF-1 deployment switch system. When ITF-1 is deployed from a rocket, two direct acting switches and two power switches are opened and the entire electric circuit is connected. The direct acting switches were made of aluminum. In the development phase of the direct acting switches, the switches were fixed and not opened. Thus, it was expected that the switches were fixed and did not open when ITF-1 deployed from the rocket.

Figure 24 shows the ITF-2 deployment switch system. Two direct acting switches were removed resulting in a simpler deployment switch system than that of ITF-1. In addition, ITF-2 deployment switch was not made of metal; thus, the possibility that the switch did not open because the metal was fixed was eliminated.

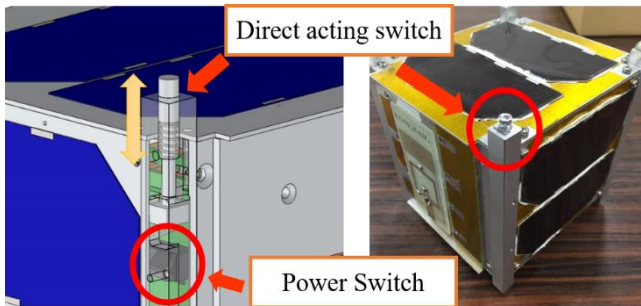


Fig. 23. ITF-1 deployment switch system

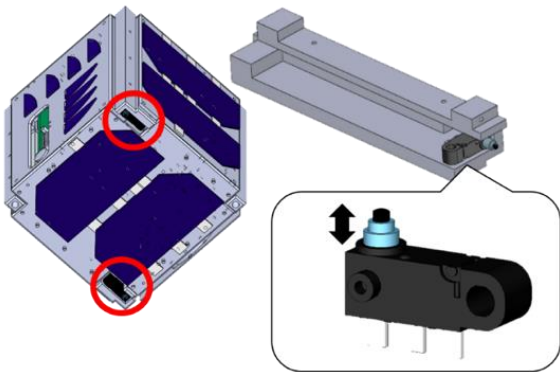


Fig. 24. ITF-2 deployment switch system

**2.4.5. Flight pin**

Figure 25 shows the ITF-1 flight pin. A circuit was

connected when this pin was put into a connector. This pin was keyed in when ITF-1 was handed over. In the EM vibration test, the flight pin had dropped off. Thus, it was considered that the flight pin dropped off during a launch and the circuit was not connected.

Figure 26 shows the ITF-2 remove before flight (RBF) pin. A circuit was connected when the RBF pin was not plugged but removed. The possibility that a circuit is not connected because the pin dropped off is essentially eliminated.

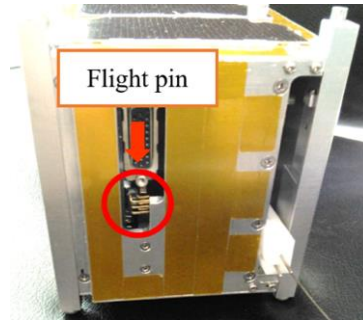


Fig. 25. ITF-1 flight pin

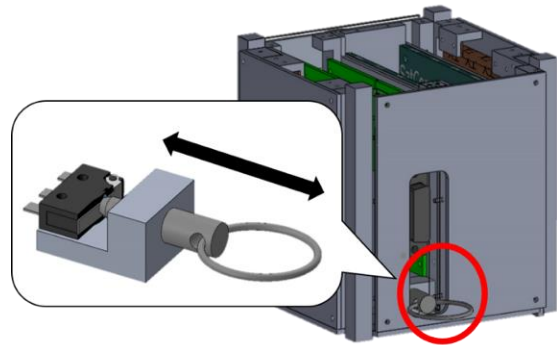


Fig. 26. ITF-2 remove before flight (RBF) pin

**2.4.6. DC/DC converter**

The DC/DC converter of ITF-1 supplied power to three transceivers. If the DC/DC converter were damaged, power would no longer be supplied to transceivers and signals would not be transmitted; thus, it was a single-point failure.

In Fig. 14, three DC/DC converters were loaded on ITF-2 and each communication system had one or more DC/DC converters such that the possibility that each DC/DC converter becomes a single-point failure was eliminated.

**2.4.7. Battery**

A consumer Li-ion battery was loaded on ITF-1 into which a protection circuit was built. In the EM vibration test, the protection circuit dropped off. Thus, it was considered that the protection circuit dropped off due to rocket vibration.

ITF-2 also loads a consumer Li-ion battery; however, its protection circuit is self-produced. It controls the overcurrent, overcharge, and over discharge of the battery. The battery and the protection circuit were set separately and securely as shown in Fig. 27. In addition, we checked carefully to ensure that these would not be damaged and dropped off by vibration.



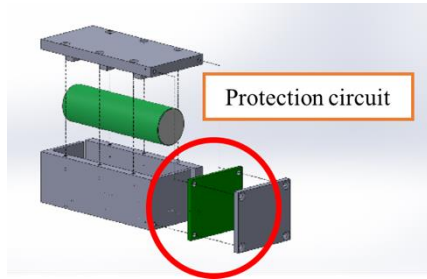


Fig. 27. Battery protection circuit of ITF-2.

#### 2.4.8. Solar cell

ITF-1 Flight Model was launched with incorrect connection of solar cells. ITF-1 used 40 mm x 80 mm TJ GaAs solar cells, which were the same cells used in ITF-2 and the connection of one panel was 2 serials and 1 parallel. A solar cell consists of a positive electrode, a negative electrode, and bypass diode. It is necessary to connect the positive electrode and negative electrode; however, the positive electrode and the bypass diode were connected. The connection of ITF-1 was also adopted for ITF-2 and it was revealed that the power generation of the solar cells was reduced by approximately half compared to the specification of the catalog spec because of the connection on ITF-1, and hence, ITF-2 was incorrect. Furthermore, this was discovered after the solar cells were already attached on all panels with an adhesive. Therefore, we removed all cells by soaking the panels in acetone solution for approximately 10 days in a glass case as shown in Fig. 28. After the removal, the solar cells were connected again in the right connection and it was confirmed that these panels generated expected power.



Fig. 28. Removal of solar cells by soaking in acetone solution in a glass case for about 10 days.

### 3. ITF-2 operation

Figure 29 shows the operation sequence of ITF-2 from launch to re-entry. The operation sequence is divided into four phases: from launch to deployment, initial operation, system verification operation, and normal operation. In this section, the operation results as of September 2017 will be reported.

#### (1) From launch to deployment

ITF-2 was not deployed immediately after launch but was stored aboard at the ISS for a month. During the storage period, the ground station to operate ITF-2 was prepared. It was

requested that universities in Japan prepare to receive signals from ITF-2, and publish information received at both domestic and overseas HAMS through JAMSAT and AMSAT. Figure 30 shows the moment of the satellite's deployment using the JEM Small Satellite Orbital Deployer (J-SSOD) system. After 30 min from the deployment, the monopole antenna was deployed and ITF-2 began transmitting RF radiation. A CW downlink was received and it successfully achieved uplink from the ground station within one day of deployment.

#### (2) Initial operation period

During the initial operation period, the health of the satellite bus systems, the balance of power supply, and power consumption, and the health of each communication system were checked. We were not able to receive signals from communication system B with ultra-small antenna; however, we checked all items except communication system B. Achieving an uplink and downlink with communication system B was one of ITF-2's missions; thus, it was decided to continue to check it until re-entry of ITF-2 and the completion of the initial operation.

#### (3) System verification operation period

During system verification operation, we checked whether ITF-2 handled uplink commands and downlink messages using each radio waves, changed registered messages, and downlinked at scheduled time, and so on, and the system verification operation was successfully completed.

#### (4) Normal operation period

During normal operation, the satellite was operated to achieve its missions. In previous operation, the basic downlink cycle, which was a cycle of 10 s CW transmission and 90 s of reception, as well as downlinks of HK data and messages with F2A and F2D during periods when ITF-2 passed over Japan, were operated. In normal operation, the amount of time in which ITF-2 transmitted F2A and F2D around the world in order to promote reception reports from overseas was increased.

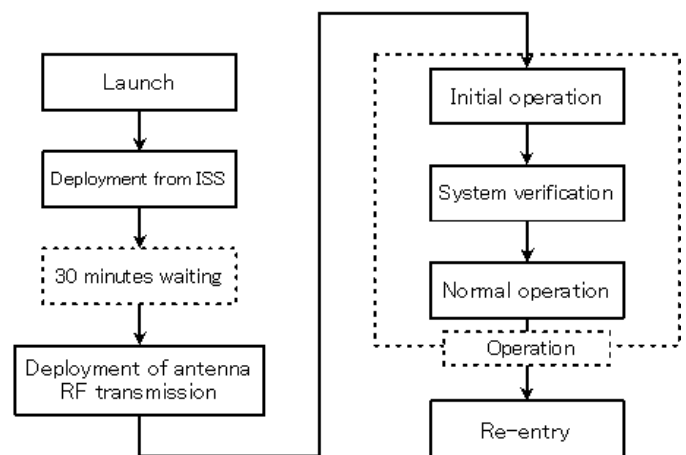


Fig. 29. Operation sequence of ITF-2



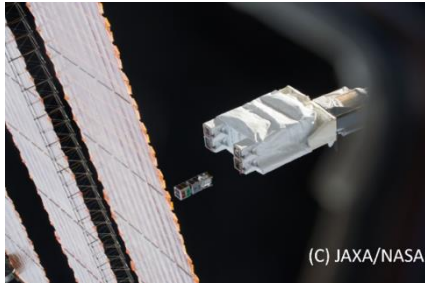


Fig. 30. Deployment of satellites from ISS. Left satellite is ITF-2.



Fig. 33. SWL cards.

### 3.1. Status of achievement of missions

#### (1) The construction of YUI network

As of September 2017, more than 900 reception reports by HAMs from 19 countries were reported. The latest reception reports were posted on the ITF-2 operation web page. These results show the success of promoting receptions from HAMs. On the other hand, there were few reception reports from people not normally involved in amateur radio. It is necessary to promote this mission to facilitate their interest in receiving signal from ITF-2. As examples of the current promotion, an original web report form that allows people to enjoy reporting in a simple manner was provided (Fig. 31), and events were held where people can enjoy receiving signals from ITF-2 with simple and low-cost handmade antenna (Fig. 32). Furthermore, short wave listener (SWL) cards were sent to people who receive signals from ITF-2 and report it along with their report's written contents (Fig. 33). The web report form was written in Japanese and English, and enables people to check the current status of ITF-2 based on data reported. SWL cards were provided to participants of reception experience events, people who have reported receiving signals from ultra-small antenna, and so on. These activities provide opportunities to experience receiving satellite signals.

#### (2) Demonstration of ultra-small antenna

As of September 2017, signals from the ultra-small antenna were received. Figure 34 shows the CW signal received from it at the University of Tsukuba ground station. In addition, we succeeded in resetting the microcontroller using this antenna. Some reception reports of signals, which seem to have been transmitted by the ultra-small antenna, were reported locally and overseas. However, the FM downlink from this antenna has not been successful.

The intensity of CW signal from the ultra-small antenna was weaker than signal from the monopole antenna. Ultra-small antenna has high directionality and the structure panel with ultra-small antenna does not always direct to the Earth when ITF-2 transmits signals from the ultra-small antenna because the attitude control of ITF-2 is passive with the earth's magnetism. This results in less success in terms of downlink and uplink with the antenna. Based on these reasons, it is necessary to improve the attitude control system and gain of the ultra-small antenna such that it can be used as the main antenna.

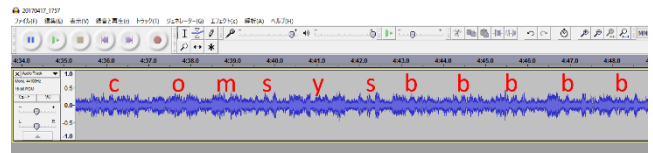


Fig. 34. Signal from ultra-small antenna received at the University of Tsukuba ground station.



Fig. 31. Original web report form.



Fig. 32. Receiving experience event.

#### (3) Demonstration of new microcontroller

The count data was stored in an electrically erasable programmable read-only memory (EEPROM). The command data was also memorized in it. If the count of SEL and SEU are over 255, the counter is reset and starts counting from 0 again. However, the counts have gone down since April 2017. Possible factors for this are the degradation of the EEPROM, the reset command from the ground station, the periodic reset every 12 h or other factors may have caused it to delete. In fact, some commands were deleted by a reset command and have been disabled since April 2017.

## 4. Conclusion

In this paper, an overview and five systems of ITF-2 were introduced, namely power supply, communication, command and data handling (C&Dh), thermal and structure, and attitude control. In addition, the ITF-2 design change from the expected

defects of ITF-1 were also introduced: antenna deployment mechanism, receiver, microcontroller, deployment switch, flight pin, DC/DC converter, battery and solar cell.

In addition, we reported the operation results as of September 2017. CW downlinks and uplinks to ITF-2 were successful within one day of deployment, and the operation sequence to normal operation was introduced. The status of mission achievement were also reported. (1) Development of the YUI network. More than 900 reception reports by HAMs from 19 countries were reported, indicating the success of the outreach to HAMs. On the other hand, there were few reception reports from people who were not usually involved in amateur radio. It is necessary to promote this mission further to allow them to develop interest in receiving signals from ITF-2. (2) Demonstration of the ultra-small antenna. CW signals from ultra-small antenna were received and we succeeded in resetting the microcontroller using this antenna. FM downlink from this antenna has not been successful. The attitude control system and the gain of the ultra-small antenna should be improved so that the ultra-small antenna can be used as the main antenna. (3) The number of SEL and SEU that have occurred in MSP430FR5739 (MSP) from January 2017 to September 2017 was reported. However, the counts have gone down since April 2017. Possible factors for this are the reset command from the ground station, the periodic reset every 12 h or other factors may have caused it to delete due to the degradation of EEPROM.

## Acknowledgments

We are grateful to officials of the JAXA for the deployment and achievement of the missions of ITF-2. We were able to use unique equipment, airlock and robot arm, and we had the opportunity to deploy small satellites from Kibo, start missions by using Kibo, and receive flexible responses to our needs and schedule for the launch and deployment.

In addition, we are grateful for the development and economic supports from antenna 1st, Ryohei Technica Corporation and supporters of crowd-funding.

## References

- 1) University of Tsukuba YUI project HP, <http://yui.kz.tsukuba.ac.jp/>, 2017 (accessed April 23, 2017).
- 2) Akagi, H., Takata, M., Watanabe, H., and Oikawa, K.: *Kibo's contribution to broadening the possibilities for Micro/Nanosatellite*, Proceedings of the SpaceOps 2016 Conference, Daejeon, Korea, May 16-20, 2016, AIAA 2016-2517.
- 3) Seri, Y., Masui, H., and Cho, M.: *Mission Results and Anomaly Investigation of HORYU-II*, 2013.
- 4) Tsuda, Y., Sako, N., Eishima, T., Ito, T., Arikawa, Y., Miyamura, N., Tanaka, A., and Nakasuka, S.: *University of Tokyo's CubeSat project: its educational and technological significance*, 2001.
- 5) Shibagaki, R.: *Development and verification of power supply system onboard High Voltage Technology Demonstration Satellite HORYU-II*, HORYU KIT Satellite Project HP List of papers, 2012, <http://kitsat.ele.kyutech.ac.jp/horyu2/documents.html> (in Japanese) (accessed October 30, 2017).
- 6) ITF-2 operation web page, <https://operationitf-2.blogspot.jp/>, 2017 (accessed April 23, 2017).